Solid State Communications 148 (2008) 361–364

Contents lists available at ScienceDirect

Solid State Communications

journal homepage: www.elsevier.com/locate/ssc

Effects of pressure on electrical property of $BaIrO_3$

J.G. Zhao *, L.X. Yang, K. Mydeen, F.Y. Li, R.C. Yu, C.Q. Jin

Beijing National Lab for Condensed Matter Physics, Institute of Physics, Chinese Academy of Sciences, Beijing 100190, PR China

ARTICLE INFO

Article history:
Received 6 August 2008
Received in revised form
14 September 2008
Accepted 23 September 2008 by D.D. Sarma
Available online 1 October 2008

PACS:
62.50.+p
72.80.Ga
71.30.+h
75.50.Dd

Keywords:
A. Barium iridate
D. Weak itinerant ferromagnetism
E. High-pressure effect

ABSTRACT

The *in situ* high-pressure measurements of electrical resistivity versus temperature for weak ferromagnetic $BaIrO_3$ have been performed, using a Cu–Be piston–cylinder-type apparatus up to 1.0 GPa at 80–300 K. The electrical resistivity is increasing with pressure. The pressure derivative of Curie temperature $\partial T_c/\partial P$ is equal to −6.1(2) K/GPa, and the relative pressure dependence $\partial \ln T_c/\partial P$ is equal to −3.4(1)%/GPa, which indicates that $BaIrO_3$ is a weak itinerant ferromagnet.

1. Introduction

At ambient pressure, $BaIrO_3$ crystallizes into the distorted 9R $BaRuO_3$ structure [1], with the space group $C2/m$, due to a large tolerant factor (about 1.051) as calculated from the ion radii in Shannon Table [2]. The schematic view of the crystal structure is shown in Fig. 1. $BaIrO_3$ is a weak ferromagnet [3,4], with the Curie temperature T_c about 183 K. It is the first known ferromagnet that contains a 5*d* transition metal cation in a ternary oxide, which originates from spin polarization of Ir cations rather than spin canting [5,6]. The polycrystalline sample of $BaIrO_3$ is a semiconductor [7]. The obvious kink in the ρ–T curve corresponds to the Curie temperature T_c. Blow T_c, the electrical resistivity increases more rapidly with the decreasing temperature. For the single crystal, the temperature dependence of resistivity in the *ab*-plane is similar with that of the polycrystalline $BaIrO_3$, but the electrical resistivity at low temperature is much smaller than the corresponding value of polycrystal at the same temperature [5]. However, along the *c*-axis that is the high conductivity axis, $BaIrO_3$ transforms to a more insulating phase below T_c, and then transforms to metallic and insulating states at 80 K and 26 K, respectively [5,6], which is different from the ρ–T curve of polycrystal. For $BaIrO_3$, the ρ_c is smaller than ρ_{ab}, due to direct Ir–Ir interaction along the *c*-axis. This metal–insulator transition was ascribed to the charge density wave (CDW) formation in $BaIrO_3$, where the transition temperature T_{CDW}, i.e. T_{c1} in [5], is equal to about 26 K. The CDW behavior is due to the distortion of IrO_6 octahedron in the low symmetry quasi-one-dimensional chain-type structure of $BaIrO_3$, which reduces the bandwidth and enlarges the band gap.

Pressure is an important thermodynamical parameter to control the matter state. The knowledge about the pressure behavior is very helpful to fully understand the overall properties of materials. High pressure can affect the magnetic properties of oxide ruthenates, e.g. $SrRuO_3$ [8], Ca_2RuO_4 [9]. The T_c of $SrRuO_3$ is decreasing with increasing pressure by measuring electrical resistivity and AC magnetic susceptibility [8]. The pressure results and DC magnetization indicate that $SrRuO_3$ is a moderately weak itinerant ferromagnet. Ca_2RuO_4 becomes a ferromagnetic metal at 0.5 GPa from an antiferromagnetic Mott insulator, due to the phase transition from S-*Pbca* to L-*Pbca* structures under high pressure [9]. The discontinuity at 0.5 GPa in the relationship of electrical resistivity versus pressure indicates the first-order insulator–metal transition in Ca_2RuO_4. To our knowledge, there are no reports of high-pressure properties for oxide iridates so far. So it is interesting to learn how physical properties of iridates will evolve under pressure. Here we report the effects of pressure on electrical property of $BaIrO_3$, using *in situ* high-pressure measurements of resistivity versus temperature in a Cu–Be piston–cylinder-type apparatus.

* Corresponding author. Tel.: +86 10 82648041; fax: +86 10 82640223.
E-mail address: zhaojinggeng@163.com (J.G. Zhao).

0038-1098/$ – see front matter © 2008 Elsevier Ltd. All rights reserved.
doi:10.1016/j.ssc.2008.09.043

2. Experimental

$BaIrO_3$ was synthesized by using the method of conventional solid-state chemical reaction. The starting materials were barium carbonate and iridium metal of 99.9% purity. Stoichiometric quantities of materials were mixed together, ground about 30 min in an agate mortar, and placed into an Al_2O_3 crucible. Then the powder was calcined for about 12 h at 900 °C in air. The calcined powder was reground, pressed into a pellet at the pressure of 10 MPa, and sintered at 1000 °C for about 72 h in air with two intermediate re-grindings.

In order to obtain a high-quality $BaIrO_3$ bulk, we used a conventional cubic-anvil type high-pressure facility to perform the cold-pressing treatment. The $BaIrO_3$ powders were reground and pressed into pellets of 5.0 mm diameter, and then wrapped in silver foil to avoid contamination. The pellets were put into the hole of pyrophyllite, which was used as the pressure-transmitting medium. The treating process was carried out at 5.0 GPa about 10 min. After pressure release, the pellets were sintered at 1000 °C for about 24 h in air in order to let the grains grow. This method has obviously improved the sample's property [10,11].

The prepared sample was checked by the powder x-ray diffraction (XRD) with CuK_α radiation at room temperature, using a Rigaku diffractometer (MXP-AHP18). The experimental data were collected in 2θ-steps of 0.02° and 3 s counting time in the range 10^Ω–120^Ω and analyzed with Rietveld method by using the FullProf program [12]. The XRD pattern indicates that our $BaIrO_3$ sample is a single phase. The relationship between magnetic susceptibility and temperature was obtained using a SQUID magnetometer (Quantum Design, MPMS-5S) in the range 5–300 K. Data were collected under both zero-field-cooled (ZFC) and field-cooled (FC) conditions in an applied field of 0.1 T. The temperature dependence of electrical resistivity in the range 5–300 K at ambient pressure was obtained using the four-probe method with Ag paste contacts on an Oxford Maglab measuring system.

A piston–cylinder-type apparatus, being made of the alloy of copper and beryllium, was used to perform the *in situ* high-pressure measurements of resistivity versus temperature. In order to keep a good hydrostatic environment, a kind of mixed silicon oil and kerosene was used as the pressure-transmitting medium. The pressure is calibrated by measuring the well known superconducting transition temperature T_c of lead metal. The low-temperature experiments were carried out in a Dewar and the temperature was read from a NiCr–NiAl thermocouple. The electrical resistivity of sample was obtained by the conventional four-probe method with Ag paste contacts at 0.0–1.0 GPa from the liquid-nitrogen temperature to ambient.

3. Results and discussion

Fig. 2 shows the observed and fitted XRD patterns of $BaIrO_3$, and the inset shows the details in the range 70°–120°. The data are fitted with the $C2/m$ space group and analyzed with the Rietveld method. The obtained R_p, R_{wp}, and R_{exp} factors are 6.18%, 8.19%, and 4.88%, respectively, which indicates the good consistence of the refined results. The lattice parameters are refined to be $a = 10.0064(2)$ Å, $b = 5.7518(1)$ Å, $c = 15.1668(2)$ Å, and $\beta = 103.278(1)°$. Table 1 lists the Wyckoff notation, atomic coordinates, and thermal parameters. The XRD data indicate that the sample is good for the further research in the electrical and magnetic properties.

Fig. 3 shows the temperature dependence of magnetic susceptibility for $BaIrO_3$. The result is similar with that of the polycrystalline sample in Ref. [4]. According to the χ–T curve, $BaIrO_3$ is a weak ferromagnet at low temperature, with the Curie temperature T_c 183.8 K. The ZFC curve is same with the FC curve above T_c, but

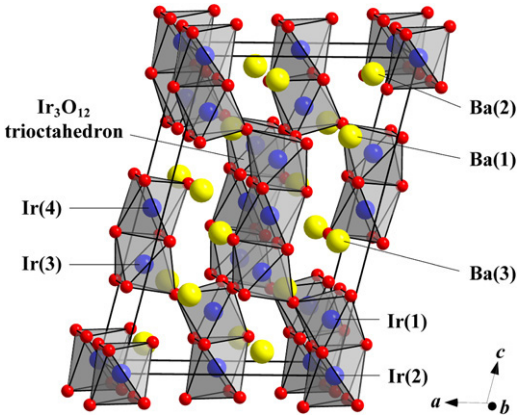

Fig. 1. The schematic view of the crystal structure of $BaIrO_3$. Here the IrO_6 octahedrons are represented by geometrical figures (Ir at the center, O at corners), and the Ba cations are described as circles. The unit cells are outlined.

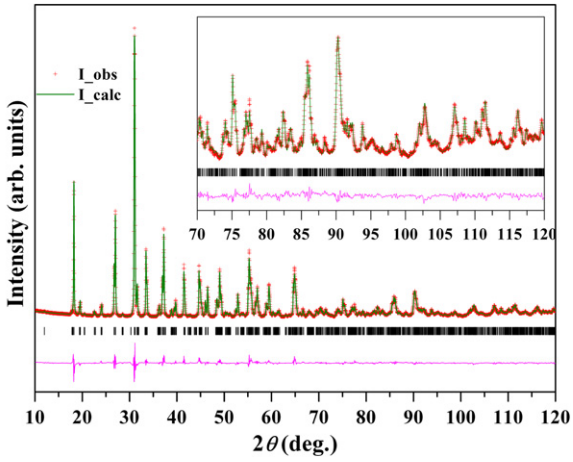

Fig. 2. The experimental (open circle) and fitted (line) x-ray diffraction patterns for $BaIrO_3$. The difference plot between observed and calculated patterns is shown at the bottom. The positions of the Bragg reflections are shown by the vertical lines. The inset shows the details of patterns in the range 70°–120°.

Table 1
Wyckoff notation, atomic coordinates, and thermal parameters for $BaIrO_3$.

Atom	Site	x	y	z	B (Å^2)
Ba(1)	4i	0.7779(3)	0	0.2506(3)	0.68(5)
Ba(2)	4i	0.3693(3)	0	0.0731(2)	0.72(6)
Ba(3)	4i	0.1511(3)	0	0.4237(2)	0.69(6)
Ir(1)	4i	0.0847(2)	0	0.1766(1)	1.25(4)
Ir(2)	2a	0	0	0	1.04(6)
Ir(3)	4i	0.4657(2)	0	0.3217(1)	1.20(4)
Ir(4)	2d	0	0.5	0.5	1.16(6)
O(1)	4i	0.284(2)	0	0.232(2)	1.4(6)
O(2)	8j	0.071(1)	0.271(3)	0.270(1)	2.1(3)
O(3)	4i	0.879(4)	0	0.110(2)	3.2(9)
O(4)	8j	0.135(2)	0.296(5)	0.075(2)	3.4(8)
O(5)	8j	0.395(1)	0.236(3)	0.399(1)	3.4(3)
O(6)	4i	0.649(2)	0	0.423(2)	2.0(5)

deviates from FC curve below T_c, due to the rapid zero-field cooling [4]. The relationship of reciprocal magnetic susceptibility versus temperature, as shown in the inset of Fig. 3, is not linear in the paramagnetism region. So the χ data above T_c should be fitted to the following modified Curie–Weiss law:

$$\chi = \frac{C}{T-\theta} + \chi_0, \tag{1}$$

where the parameters C, θ, and χ_0 are the Curie constant, paramagnetic Curie temperature, and the temperature independent mag-

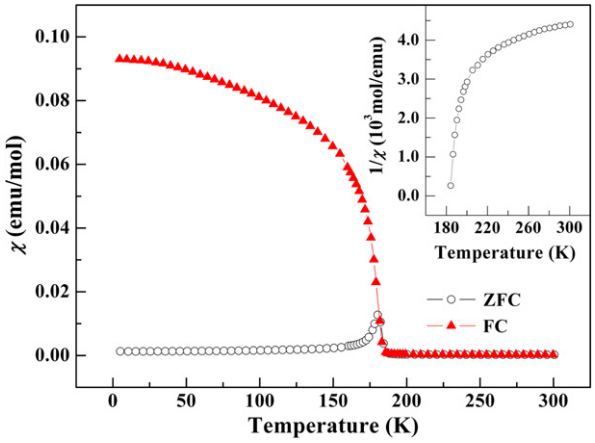

Fig. 3. Temperature dependence of magnetic susceptibility for $BaIrO_3$ in the range 5–300 K. The inset shows the relationship between reciprocal magnetic susceptibility and temperature above T_c for the ZFC mode.

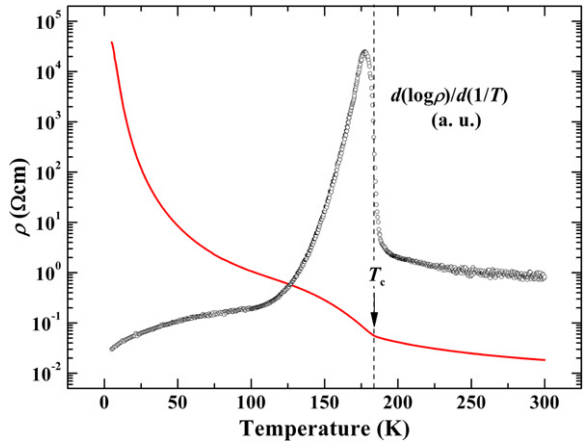

Fig. 4. Temperature dependence of electrical resistivity (solid line) and the derivative $d(\log \rho)/d(1/T)$ (open circle) for $BaIrO_3$ in the range 5–300 K, where $d(\log \rho)/d(1/T)$ is in arbitrary units.

netic susceptibility, respectively. The paramagnetic Curie temperature θ of 183.7(2) K is positive, which is consistent with the weak ferromagnetism of $BaIrO_3$. The effect magnetic moment per formula unit (μ_{eff}) of 0.127(3) μ_B, as obtained from C through the formula $\mu_{eff} = 2.83\sqrt{C}$, is approximately equal to the value in Ref. [5]. μ_{eff} is less than the theoretic value of about 1.73 μ_B calculated in the spin-only model for one unpaired 5d electron in the Ir^{4+} cations. The small μ_{eff} indicates that the Ir^{4+} cation loses partly local moment, which is attributed to the strong spin-orbit coupling in Ir cations and the improved itinerancy resulting from the direct interaction between two adjacent Ir cations in the Ir_3O_{12} trioctahedron that lowers the magnetization of the sample.

Fig. 4 shows the temperature dependence of the electrical resistivity $\rho(T)$ (solid line) and the derivative $d(\log \rho)/d(1/T)$ (open circle) for $BaIrO_3$. The ρ–T curve is similar with the previous result of polycrystalline sample [7]. It is clear that $BaIrO_3$ is a semiconductor, with the electrical resistivity about $10^5\Omega$ cm at 5 K. There is an obvious kink in the ρ–T curve, corresponding to the Curie temperature T_c, which is indicated by the arrow in Fig. 3. The T_c of ferromagnetism was defined as the turning point at the peak of $d(\log \rho)/d(1/T)$–T curve as shown in Fig. 4. Using this definition, the T_c is about 183.3 K for the sample, which is approximately equal to the value obtained from χ–T curve. While temperature is smaller than T_c, the electrical resistivity increases more rapidly with decreasing temperature, due to the gap open [5]. The electrical property of $BaIrO_3$ is closely related to its structure in terms of the IrO_6 octahedron connection. The Ir–Ir–Ir trimer in the trioctahedron of $BaIrO_3$ results in the novel electronic state. The wave function of the 5d orbitals is highly extended comparing with 3d ones, so the oxide iridates should be metallic, like the corresponding ruthenates. However, although the short Ir–Ir distance in the Ir_3O_{12} trioctahedron is propitious to metallic behavior, $BaIrO_3$ is not a metal [5,7]. The twisting and distortion of the Ir_3O_{12} trioctahedron reduce the bandwidth, and result in the non-metallic behavior in $BaIrO_3$ [5].

Fig. 5(a) shows the temperature dependence of electrical resistivity in the range 100–250 K at various pressures up to 1.0 GPa for $BaIrO_3$. The electrical resistivity is increasing with pressure in the experimental temperature range. When temperature is 200 K, electrical resistivity is 41.77 mΩ cm, 50.98 mΩ cm and 62.29 mΩ cm at 0.0 GPa, 0.5 GPa and 1.0 GPa, respectively. In the Ir_3O_{12} trioctahedron of $BaIrO_3$, the direct Ir–Ir distances are shorter than the separation in iridium metal (2.72 Å) [1]. From the large bulk modulus of metal iridium [13], it could be deduced that there is a strong repulsion between the two neighboring Ir cations. Pressure strengthens the repulsion between Ir cations due

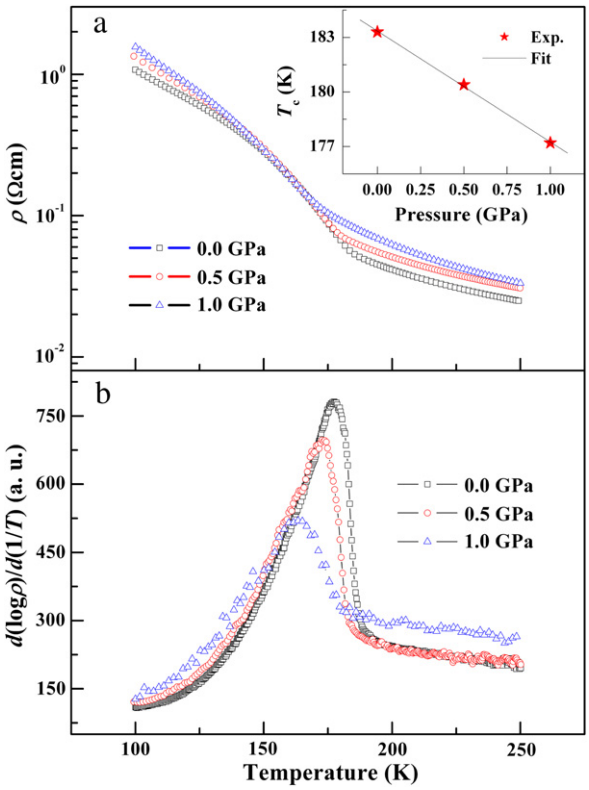

Fig. 5. Temperature dependence of (a) electrical resistivity and (b) the derivative $d(\log \rho)/d(1/T)$ at various pressures for $BaIrO_3$. The inset of (a) shows the pressure dependence of Curie temperature T_c.

to the shrinkage of crystal lattice, and then enhances the structural distortion, which enlarges the gap and results in the increase of electrical resistivity. Fig. 5(b) shows the temperature dependence of the derivative $d(\log \rho)/d(1/T)$ in the temperature range of 100-250 K at 0.0–1.0 GPa for $BaIrO_3$. According to the $d(\log \rho)/d(1/T)$—T curves, the relationship of T_c versus pressure is obtained, as shown in the inset of Fig. 5(a). The obtained Curie temperatures are 183.3 K, 180.4 K and 177.2 K at 0.0 GPa, 0.5 GPa and 1.0 GPa, respectively. T_c is decreasing with increasing pressure. The suppression of ferromagnetism transition temperature of $BaIrO_3$ is similar with that of $SrRuO_3$ [8], which can be attributed to the augment of distortion under high pressure. For the $Ba_{1-x}Sr_xIrO_3$ series, T_c is decreasing with the decreasing lattice parameter,

i.e. the increasing Sr content x [14], which is consistent with the pressure effect in this paper. In the experimental pressure range, the pressure dependence of T_c is roughly linear. The pressure derivative of the Curie temperature $\partial T_c/\partial P$ of $-6.1(2)$ K/GPa is approximately equal to the value of -6.2 ± 1.9 K/GPa for $SrRuO_3$ [8].

According to the Wohlfarth theory [15,16], the relative pressure dependence $\partial \ln T_c/\partial P$ for an homogeneous ferromagnet can approximately be expressed as

$$\partial \ln T_c/\partial P = -\alpha/T_c^2 + (5/3)\kappa, \quad (2)$$

where α is a slowly varying quantity and κ is the compressibility. For the weak itinerant ferromagnet, the $\partial \ln T_c/\partial P$ is negative, because both α and κ are positive, and the first term on the right-hand side in Eq. (2) is dominating comparing with the second term [15]. So the Curie temperature is decreasing with increasing pressure. The $\partial \ln T_c/\partial P$ of $-3.4(1)$%/GPa for $BaIrO_3$ is approximately equal to that of $SrRuO_3$ (about -3.5%/GPa) [8], but is much smaller than that of the Laves phase compound $ZrZn_2$ (about -86%/GPa) [17]. The small $\partial \ln T_c/\partial P$ supports that $BaIrO_3$ is a weak itinerant ferromagnet.

4. Conclusion

In summary, we observed the influence of pressure on the electrical property for $BaIrO_3$ through the *in situ* measurements of the temperature dependence of electrical resistivity at various pressures. The electrical resistivity is increasing with the increasing pressure and Curie temperature T_c is depressed by high pressure. The small relative pressure dependence $\partial \ln T_c/\partial P$ shows the weak itinerant ferromagnetism of $BaIrO_3$.

Acknowledgements

We thank Prof. C. Dong and H. Chen of Institute of Physics, Chinese Academy of Sciences for their help in XRD measurement and analysis, and the support from NSF and Ministry of Science and Technology of China through the research projects.

References

[1] T. Siegrist, B.L. Chamberland, J. Less-Common Met. 170 (1991) 93.
[2] R.D. Shannon, Acta Crystallogr. A32 (1976) 751.
[3] R. Lindsay, W. Strange, B.L. Chamberland, R.O. Moyer Jr., Solid State Commun. 86 (1992) 759.
[4] A.V. Powell, P.D. Battle, J. Alloys Compd. 191 (1993) 313.
[5] G. Cao, J.E. Crow, R.P. Guertin, P.F. Henning, C.C. Homes, M. Strongin, D.N. Basov, E. Lochner, Solid State Commun. 113 (2000) 657.
[6] T. Nakano, I. Terasaki, Phys. Rev. B 73 (2006) 195106.
[7] N.S. Kini, A. Bentien, S. Ramakrishnan, C. Geibel, Physica B 359–361 (2005) 1264.
[8] J.J. Neumeier, A.L. Cornelius, J.S. Schilling, Physica B 198 (1994) 324.
[9] F. Nakamura, Y. Senoo, T. Goko, M. Ito, T. Suzuki, S. Nakatsuji, H. Fukazawa, Y. Maeno, P. Alireza, S.R. Julian, Physica B 329–333 (2003) 803.
[10] J.-S. Zhou, J.B. Goodenough, B. Dabrowski, Phys. Rev. B 67 (2003) 020404(R).
[11] J.-S. Zhou, J.B. Goodenough, B. Dabrowski, Phys. Rev. Lett. 94 (2005) 226602.
[12] R.A. Young, The Rietveld Method, IUCr/OUP, Oxford, 1995.
[13] K. Gschneidner Jr., Solid State Phys. 16 (1964) 275.
[14] G. Cao, X.N. Lin, S. Chikara, V. Durairaj, E. Elhami, Phys. Rev. B 69 (2004) 174418.
[15] E.P. Wohlfarth, in: J.S. Schilling, R.N. Shelton (Eds.), Physics of Solids Under High Pressure, North-Holland, Amsterdam, 1981, p. 175.
[16] E.P. Wohlfarth, J. Phys. C 2 (1969) 68.
[17] T.F. Smith, J.A. Mydosh, E.P. Wohlfarth, Phys. Rev. Lett. 27 (1971) 1732.